Optica Applicata, Vol. IX, No. 3, 1979

Single-beam two-colour detector

JAN WITOLD BARAN, JÓZEF PIOTROWSKI, IRENA ZIMNOCH-HIGERSBERGER
Institute of Technical Physics, Military Academy of Technology, Warsaw, Poland.

A new type of photovoltaic two-colour detector composed of two junctions (e.g. p–n junctions, heterojunctions, metal–semiconductor junctions) connected in a back-to-back system and located so that the radiation passes consecutively through each of them has been examined. The short wavelength radiation is absorbed mainly in the direct incidence junction region, while the long wavelength radiation is absorbed in both the junctions. The detector operation has been considered under the conditions of the weak and strong incident signal, respectively. In the case of radiation of small intensity the two-colour operation of the detector can be achieved only by applying an external system dividing the voltage from both the junctions. At strong radiation the differential signal voltage depends only on the spectral composition of the radiation. Basic parameters of the thermal radiation detector have been evaluated, the latter being produced of silicon and designed for operation in two-colour pyrometry.

Introduction

In many cases the spectral composition of the electromagnetic radiation should be evaluated, e.g. when monitoring the temperature of the heated bodies (on the base of their emission spectrum) as well as the chemical composition of a substance (on the base of the characteristic transmission or reflection spectra). In such case the application of two-colour method allows to avoid many errors caused by the specificity of the examined object, the effect of the transmitting surrounding, the optics used, and so on.

In the nondispersive methods a set of two parallelly joined selective detectors is usually applied, each of them being in the most cases composed of a nonselective detector and respective band filters. The examined beam should be, however, split (in time or space). In the work [1] a simple two-colour detector has been proposed, which does not require the application of sets of detectors and filters. This paper presents the results of analysis and experimental examinations for this type of detectors.

Principle of the device operation

Fig. 1 presents a detector scheme examplified by an element with metal–semiconductor junctions. On the mutually opposite surfaces of the semiconductor the junctions are produced using metals creating a potential

barrier with the semiconductor. In the spectral region to which the detector is supposed to be sensitive at least one of the metalic layers is transparent. The radiation falls onto the detector from the transparent layer side. The thickness of the region between the junctions is considerably greater than the doubled diffusion length. The short wavelength

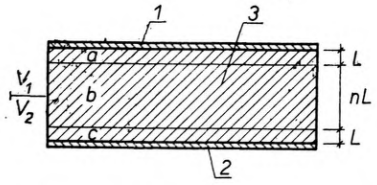

Fig. 1. Detector scheme with the metal-semiconductor junctions:
1; *2* – layers of the barrier creating metal, *3* – semiconductor, *a*; *c* – active photoelectric parts of the semiconductor material, *b* – non-active electric part

radiation ($h\nu - Eg \gg KT_D$, where T_D – detector temperature, Eg – energy gap of the used semiconductors, $h\nu$ – photon energy) is absorbed practically completely in the region *a* and does not penetrate the inside of the material. The radiation of longer wavelength ($h\nu \gtrsim Eg$) is absorbed only partly in the region *a*, a part of this radiation being absorbed in the non-active region *b* and in the region *c*. Finally the longwave radiation ($h\nu \leqslant Eg$) passes through the material being practically unabsorbed.

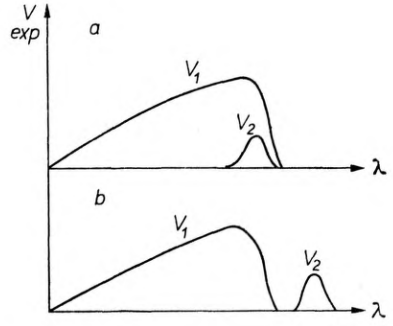

Fig. 2. The shape of the spectrum response of the detector:
a – uniform detector, *b* – semiconductor with energy gap diminishing along the direction of radiation propagation

The radiation absorbed in the semiconductor generates electron-hole pairs which, if generated in active regions, can reach space charge layers of the junctions. This evokes the appearence of the voltages V_1 and V_2 with respect to the non-active region.

The phenomena described cause the spectral characteristics of the junctions of the form shown qualitatively in fig. 2a. The position of the

spectral response maximum of the junction *2* is shifted toward greater wavelengths. Using a semiconductor with the energy gap diminishing along the direction of radiation as a detector material, we may obtain the spectral response shown in fig. 2b with a strongly marked mutual shift of the sensitivity region of the both junctions.

Experimental realization of the detector

Fig. 3 presents a schema of detector production. Two-sided planar structure on the *n*-type silicon substrate is used. The plate of thickness 100–500 μm is covered with a thin SiO_2 layer by thermic oxidation. Next, 50–1000 μm diameter windows are etched on the opposite surfaces and the gold layers deposited by the method of vacuum evaporation to cre-

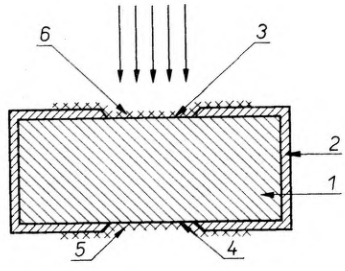

Fig. 3. Scheme of the detector performance
1 – silicon, *2* – SiO_2 layer, *3*; *4* – etched windows, *5*; *6* – gold layers

ate a barrier contact with the *n*-type silicon. The thickness of the gold layers on the incident side and its opposite amounts to about 14 and 100 nm, respectively. In the last stage the element is mounted into the body of izolator of T 29.9 type and the electric leads produced.

An analysis of detector parameters

The voltage generated by the radiation at the junctions *1* and *2* may be expressed by the formulae

$$V_1 = \frac{KT_D}{e} \ln\left(\frac{I_{\varphi_1}}{I_{s_1}} + 1\right), \tag{1}$$

$$V_2 = \frac{KT_D}{e} \ln\left(\frac{I_{\varphi_2}}{I_{s_2}} + 1\right), \tag{2}$$

where:
$I_{\varphi_1}, I_{\varphi_2}$ – currents generated by the radiation in the junctions *1* and *2*,
I_{s_1}, I_{s_2} – saturation currents of these junctions.

Case of weak generation

Let $I_{s_2} \gg I_{\varphi_1}$ and $I_{s_2} \gg I_{\varphi_2}$. The relations (1) and (2) take then the forms

$$V_1 = \frac{KT_D}{e}\frac{I_{\varphi_1}}{I_{s_1}}, \tag{3}$$

$$V_2 = \frac{KT_D}{e}\frac{I_{\varphi_2}}{I_{s_2}}. \tag{4}$$

The relations (3) and (4) show, that in this case the voltages V_1 and V_2 are proportional to I_{φ_1} and I_{φ_2}, thus proportional to the flux densities φ_1 and φ_2 of the photons absorbed in the active region of the junctions *1* and *2*. In order to obtain the quantities independent of the total radiation intensity and dependent only on the ratio N_1/N_2 (where N_1 — the number of carrier pairs generated by φ_1, and N_2 — the number of carrier pair generated by φ_2) it is necessary to carry out the dividing operation φ_1/φ_2 by means of the respective external electric system. Linear dependence of V_1 and V_2 upon the quantities φ_1 and φ_2 takes place also for great values of φ_1 and φ_2, if the junctions have been loaded with a suitably low resistance of the amplifier.

Case of strong generation

Let $I_{\varphi_1} \gg I_{s_1}$ and $I_{\varphi_2} \gg I_{s_2}$. We assume additionally that the detector load is in the form of a electronic system of sufficiently high input resistance R_w

$$R_w \frac{KT_D}{eI_{s_1}}, \frac{KT_D}{eI_{s_2}}.$$

In this case from eqs. (1) and (2) we get

$$V_1 - V_2 = \frac{KT_D}{e}\ln\left(\frac{I_{\varphi_1}}{I_{\varphi_2}}\right) + \frac{KT_D}{e}\ln\left(\frac{I_{s_1}}{I_{s_2}}\right). \tag{5}$$

Assuming the symmetry of electric properties of both the junctions ($Is_1 = Is_2$) and taking into account of the fact that

$$\frac{I_{\varphi_1}}{I_{\varphi_2}} = \frac{\varphi_1}{\varphi_2}$$

we obtain

$$V_1 - V_2 = \frac{KT_D}{e}\ln\frac{\varphi_1}{\varphi_2}. \tag{6}$$

Calculation of the parameters of the detector as pyrometer sensor

For the sake of simplicity we assume that only the carriers, generated at the distances equal to the diffusion length L from the junction regions, will be reach them by diffusion. Let the thermal radiation from a body of the temperature T fall on the detector. We assume that the condition of strong generation is fulfilled. Let the coefficient of reflection from the both surfaces be equal to zero, and let the emissivity of the hot body depend weakly upon the wavelength λ, though it may differ considerably from 1. Then

$$V = \frac{KT_D}{e} \ln \frac{\int_0^\infty E(\lambda, T)\left(1-\exp\left(-\alpha(\lambda)L\right)\right)\lambda d\lambda}{\int_0^\infty E(\lambda, T)\exp\left(-\alpha(\lambda)(n+1)L\right)\left(1-\exp\left(-\alpha(\lambda)L\right)\right)\lambda d\lambda}, \qquad (7)$$

where $E(\lambda, T)$ — denotes the Planck's distribution, α — the coefficient of absorption of the silicon detector depending upon the wavelength λ, n is related to the thickness D and the diffusion length L by the formula: $D = (n+2)L$(see fig. 1).

For numerical calculations of the integrals in the expression (7) we have assumed that the integration limits are $\lambda_1 = 0.477$ μm and $\lambda_2 = 1.144$ μm, thus they comprise the whole wavelength range within which the absorption by the extreme layers of the detectors is negligible. The diffusion length L is assumed to be 10 μm, while the dependence of the absorption coefficient α upon the wavelength has been taken from the BONNET's work [3]. The integration has been performed for 800 K $<$ 3000K and 40 μm $\leqslant D \leqslant$ 240 μm.

The operation principle of the detector as pyrometer sensor may be explained by means of the graphs presented in fig. 4. In this figure

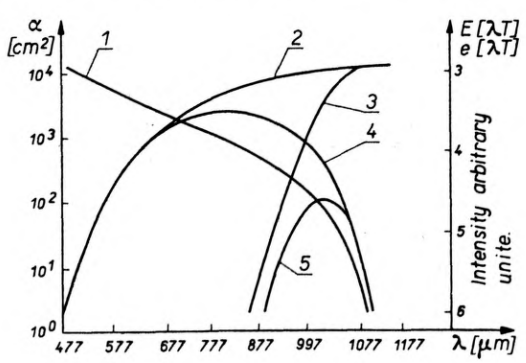

Fig. 4. The absorption coefficient vs. the wavelength for silicon (curve *1*); intensity of the radiation illuminating the first (curve *2*) and the last (curve *3*) detector layers of the thickness L, and the number of photons absorbed in the first (curve *4*) and last (curve *5*) layers of the detector, T = 1800 K, D = 140 μm

(logarithmic scale) the curve *1* presents the relation $a(\lambda)$, the curve *2* shows the radiation spectrum incident on the detector, and the curve *3* shows the radiation spectrum falling on the last detector layer of the thickness L and described by the function

$$e'(\lambda, T) = E(\lambda, T)\exp\left(-a(n+1)L\right). \tag{8}$$

The curve *4*, in turn, presents the radiation spectrum absorbed in the first layer of thickness L; while the curve *5* shows an analogical spectrum for the last layer. The last four curves are presented in the same (logarithmic) scale and refer to the temperature 1800 K and to the detector 140 μm thick. As it may be easily seen, the shape of the curves *4* and *5* is bell-like. The drop of both the curves on the long wavelength side is caused by the sharp drop of the absorption coefficient in silicon (curve *1*). The amount of the absorbed energy on the short wavelength side diminishes due to lowering of the spectral radiation intensity incident onto the layers considered. In the first layer this occurs due to short-wavelength drop of radiation of the examined body (curve *2*), while in the last layer the same results from the sharp cut-off on the short-wave-length side (due to absorption in the silicon sample) (curve *3*).

Due to difference in the spectral intensity distributions of the radiation incident on the first and the last layer the maxima of the curves *4* and *5* are shifted with respect to each other. With the change of the temperature T the position of the maximum of the curve *4* varies within $\lambda = 0.75\ \mu m \pm 0.5\ \mu m$. The maximum of the curve *5* falls on $\lambda = 1.01\ \mu m$. The operation of the detector is based on fact that in the first layer the absorbed energy increases with the temperature quicker than in the last one.

The sensitivity dependence upon the measured temperature T for the detectors of thicknesses 40 μm, 140 μm, and 240 μm is presented in fig. 5

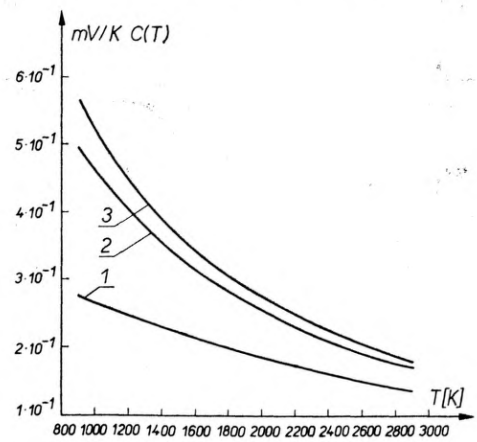

Fig. 5. The absolute sensitivity of the sensor vs. the temperature of the examined object for the detectors of thickness D = 40 μm (curve *1*), 140 μm (curve *2*), and 240 μm (curve *3*)

(curve *1*, *2*, *3*). These curves show that the sensor sensitivity drops with the increase of the temperature measured. This drop is the more nonlinear the thicker is the used silicon plate.

The curves in fig. 6 show the dependence of the sensor sensitivity C upon the silicon plate thickness for the temperatures 900 K (curve *1*), 1500 K (curve *2*) and, 2900 K (curve *3*). The sensitivity increases with the increase of the plate thickness tending to saturation. It is worth emphasizing that within the whole examined ranges of thickness and temperature the sensitivity does not drop below 0.01 mV/K.

The relative nonlinearity coefficient W of the sensor is given by the

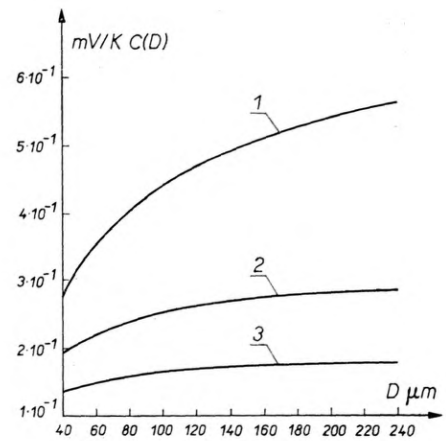

Fig. 6. The absolute sensitivity of the sensor vs. the detector thickness for the measured temperatures T = 900 K (curve *1*), 1500 K (curve *2*), and 2900 K (curve *3*)

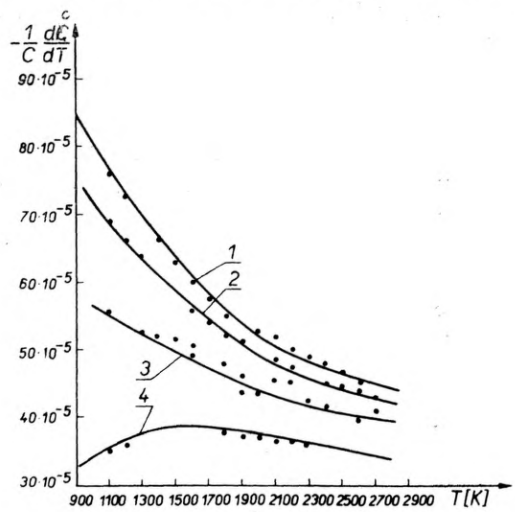

Fig. 7. Temperature dependence of the relative nonlinearity coefficient of the sensor. The curves *1–4* relate successively to detectors of thickness 240 μm, 140 μm, 80 μm, and 40 μm

formula

$$W = \frac{1}{c}\frac{dc}{dT}. \tag{9}$$

Its temperature dependence for the detectors of the thicknesses 40 μm, 80 μm, 140 μm and 240 μm has been shown in fig. 7. It is of negative value. For the great thicknesses a monotonic drop of the absolute value of this coefficient is observed. With the decreasing thickness the rate of the dropping down diminishes.

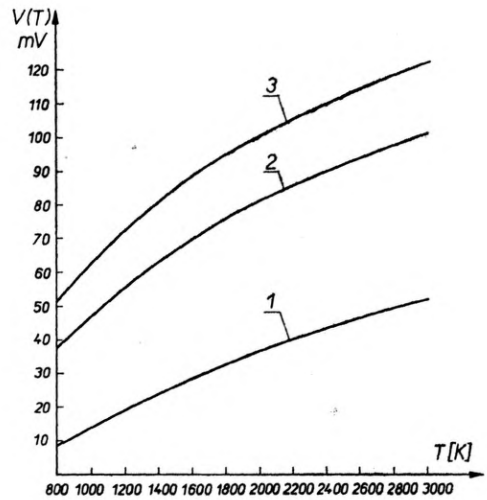

Fig. 8. The dependence of sensor signal on the temperature T measured for the detectors of the thickness D — 40 μm (curve *1*), 140 μm (curve *2*), and 240 μm (curve *3*)

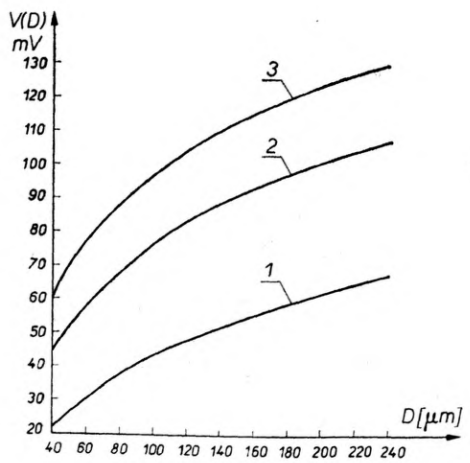

Fig. 9. The dependence of the sensor signal on the detector thickness D for the temperature measured T = 900 K (curve *1*), 1500 K (curve *2*), and 2900 K (curve *3*)

The dependences of the detector signal (in mV) on the temperature T of the examined object and thickness D of the semiconductor detector element have been presented in figs. 8 and 9, respectively. As it may be seen these values are contained within the interval 10–130 mV.

Conclusions

1. A simple device to control the spectral content of the thermal radiation has been designed, and used as a pyrometric two-colour temperature sensor.
2. The analysis of the temperature sensor has been carried for the detector made of silicon.
3. The detector sensitivity to the changes of temperature depends on the object temperature and increases with thickness of the silicon plate. The sensitivity becomes saturated practically at the plate thickness greater than 20 diffusion lengths.
4. The sensitivity of the detector suggested amount to about 0.03 mV/K and is practically sufficient to the measurement within the range of 800–3000 K.

References

[1] Igras E., Piotrowski J., Gren Z., Zimnoch-Higersberger I., Detektor dwubarwowy. Zgłoszenie patentowe P-203786.
[2] Sze M., *Physics of Semiconductor Devices*, John Wiley and Sons Inc., New York-London-Sydney-Toronto 1969.
[3] Bonnet D., *Cooperation mediterranienne pour l'énergie solarie*, Bull. No. 18, April 1970.
[4] Morgenau H., Murphy G. M., *Matematyka w fizyce i chemii*, PWN, Warszawa 1965.

Received, August 2, 1978

Однопучковый двухцветный фотовольтаический детектор

Испытывали новый тип двухцветного фотогальванического детектора, состоящего из двух пушпульно включенных переходов (электронно-дырочных переходов, гетеропереходов, контактов металлполупроводник), изготовленных таким образом, что излучение проходит последовательно через каждый из них. Коротковолновое излучение поглощается, главным образом, в области перехода, на который оно непосредственно падает, а длинноволновое излучение в обоих переходах (или в области протиположного перехода). Рассмотрена работа детектора в условиях слабого и сильного сигналов. В случае излучения малой интенсивности для достижения двухцветной работы необходимо применить внешню систему, разделяющую напряжение от обоих переходов. При сильном излучении разностное напряжение сигнала зависит только от спектрального состава излучения, не зависит же от суммарной интенсивности излучения. Вычислены основные параметры детектора термического излучения, изготовленного из кремния и предназначенного для двухцветной пирометрии.